

Use of Atomic Force Microscopy for the Study of Surface Acid–Base Properties of Carboxylic Acid-Terminated Self-Assembled Monolayers

Kai Hu and Allen J. Bard*

Department of Chemistry and Biochemistry, The University of Texas at Austin,
Austin, Texas 78712

Received January 24, 1997. In Final Form: July 11, 1997[⊗]

Atomic force microscopy was used to measure the forces between a silica probe and a carboxylic acid-terminated self-assembled monolayer (SAM) on a gold substrate in the presence of KCl electrolyte solutions of different pH. Silica–silica interaction force measurements were conducted at different pH values to determine the silica probe surface electrostatic potentials under these conditions. The interaction between two silica surfaces is repulsive and can be accurately predicted (except at short distances) by the Derjaguin–Landau–Verwey–Overbeek theory. The interaction between silica and clean gold surfaces exhibits an attractive interaction at neutral pH. The interaction between a silica probe and carboxylic acid-terminated SAM-covered gold substrate was a strong function of the pH value of the electrolyte. The surface electrostatic potentials of the surface-confined monolayers of carboxylic acid were obtained by theoretical fits of the force data to solutions of the complete nonlinear Poisson–Boltzmann equation, with the knowledge of silica probe surface potentials, at different solution pH values. The surface titration curve was obtained by correlating the surface potentials to the different electrolyte pH values. A theoretical fit to the titration curve provides the surface pK_a and an explanation for the broadening of the titration curve.

Introduction

Self-assembled monolayers (SAMs) prepared by the spontaneous chemisorption of thiolates on gold can be used to create surfaces of controlled charge, if the adsorbed molecules are terminated with an ionizable functional group. These charge-regulated monolayer surfaces are increasingly used as templates for the electrostatic adsorption of proteins,^{1,2} polypeptides,³ DNA,⁴ polyelectrolytes,⁵ metal ions, and other species.^{6–9} Control and quantitative measurement of the monolayer surface charge and potential are of both practical importance and scientific interest. In this paper we report how the diffuse double layer at the SAM-covered gold surface can be probed at nanometer separation by nanonewton force resolution with a modified tip on the cantilever of an atomic force microscope (AFM). The surface charge and potential can be determined from the force between the SAM-covered gold substrate and the tip on the AFM cantilever.

The AFM¹⁰ was initially developed as an instrument for imaging both conducting and nonconducting substrates. However, as shown by Ducker et al.,¹¹ for example, the AFM can also be used to measure interfacial forces between a particle on the cantilever and a flat surface. Such interfacial force measurements have also been

carried out using the surface forces apparatus (SFA).^{12,13} Measurements with the SFA have confirmed the main features of the Derjaguin–Landau–Verwey–Overbeek (DLVO) theory of colloid stability. A limitation of the SFA is the need for transparent and atomically smooth surfaces (usually a freshly cleaved mica surface plated with silver) to achieve accurate force–distance data. The AFM permits the extension of these surface force studies to a broader range of substrates without regard to size, structure, or transparency. In an AFM force measurement, the deflection of a microfabricated cantilever is measured as a function of its separation from a surface. Since the pioneering work of Ducker et al.,^{11,14} who monitored silica–silica interaction forces as a function of electrolyte concentration and solution pH, a wide range of substrates have been examined, including gold,¹⁵ zirconia,¹⁶ titania,¹⁷ polystyrene latex,¹⁸ and zinc sulfide.¹⁹ Dissimilar surface interactions have also been reported between silica and titania.²⁰ Most of these studies have focused on the measurement of double-layer forces between colloidal particles and clean flat substrates. We apply this methodology here to measure the double-layer forces between a colloidal particle and a SAM-covered flat substrate, so that information about the surface charge of surface-confined molecules can be probed. A related technique, chemical force microscopy, probes the adhesion

[⊗] Abstract published in *Advance ACS Abstracts*, September 1, 1997.

(1) Prime, K. J.; Whitesides, G. M. *Science* **1991**, *252*, 1164.
(2) Tarlov, M. J.; Bowden, E. F. *J. Am. Chem. Soc.* **1991**, *113*, 1847.
(3) Jordan, C. E.; Frey, B. L.; Kornguth, S.; Corn, R. M. *Langmuir* **1994**, *10*, 3642.
(4) (a) Xu, X.-H.; Yang, H. C.; Mallouk, T. E.; Bard, A. J. *J. Am. Chem. Soc.* **1994**, *116*, 8386. (b) Xu, X.-H.; Bard, A. J. *J. Am. Chem. Soc.* **1995**, *117*, 2627.
(5) Godínez, L. A.; Castro, R.; Kaifer, A. E. *Langmuir* **1996**, *12*, 5087.
(6) Li, J.; Liang, K. S.; Scoles, G.; Ulman, A. *Langmuir* **1995**, *11*, 4418.
(7) Collinson, M.; Bowden, E. F. *Langmuir* **1992**, *8*, 1247.
(8) Bharathi, S.; Yegnamaran, V.; Rao, G. P. *Langmuir* **1995**, *11*, 666.
(9) Zhou, Y.; Bruening, M. L.; Bergbreiter, D. E.; Crooks, R. M.; Wells, M. J. *Am. Chem. Soc.* **1996**, *118*, 3773.
(10) Binnig, G.; Quate, C.; Gerber, G. *Phys. Rev. Lett.* **1986**, *56*, 930.
(11) Ducker, W. A.; Senden, T. J.; Pashley, R. M. *Nature* **1991**, *353*, 239.

(12) Israelachvili, J. N.; Adams, G. E. *J. Chem. Soc., Faraday Trans.* **1978**, *74*, 975.

(13) (a) Horn, R. G.; Israelachvili, J. N. *J. Chem. Phys.* **1981**, *75*, 1400. (b) Parker, J. L.; Christenson, H. K.; Ninham, B. W. *Rev. Sci. Instrum.* **1989**, *60*, 3135.

(14) Ducker, W. A.; Senden, T. J.; Pashley, R. M. *Langmuir* **1992**, *8*, 1831.

(15) Biggs, S.; Mulvaney, P.; Zukoski, C. F.; Grieser, F. *J. Am. Chem. Soc.* **1994**, *116*, 9150.

(16) Biggs, S.; Mulvaney, P. In *Surfactant Adsorption and Surface Solubilization*; Sharma, R., Ed.; ACS Symposium Series 615; American Chemical Society: Washington, DC, 1995; pp 255–266.

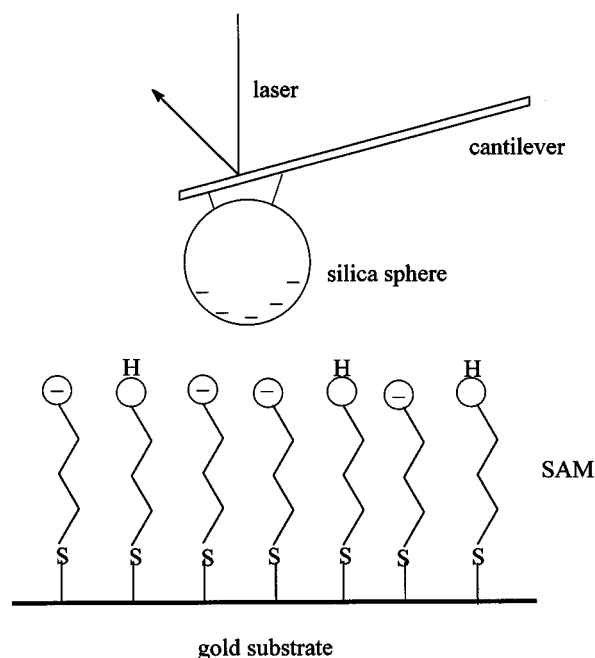
(17) Larson, I.; Drummond, C. J.; Chan, D. Y. C.; Grieser, F. *J. Am. Chem. Soc.* **1993**, *115*, 11885.

(18) Li, Y. Q.; Tao, N. J.; Pan, J.; Garcia, A. A.; Lindsay, S. M. *Langmuir* **1993**, *9*, 637.

(19) Atkins, D. T.; Pashley, R. M. *Langmuir* **1993**, *9*, 2232.

(20) Larson, I.; Drummond, C. J.; Chan, D. Y. C.; Grieser, F. *J. Phys. Chem.* **1995**, *99*, 2114.

Chart 1. Schematic of AFM Force Measurement between a Modified Spherical Tip and Carboxylic Acid-Terminated SAM-Covered Gold Substrate



forces between a chemically modified AFM tip and substrate.^{21,22}

A few techniques have previously been employed to estimate surface pK_a values for surface-confined monolayer systems at the solid–liquid interface. For example, Bain and Whitesides²³ used changes in the contact angle with pH to investigate carboxylic acid-terminated *n*-alkanethiol monolayers. Bryant and Crooks²⁴ estimated the surface pK_a values of amine-terminated monolayers by correlating the differential interfacial capacitance to the solution pH values. More recently, Kaifer and co-workers⁵ used an adsorbed viologen-based polyelectrolyte to probe the pK_a of monolayer –COOH groups. All of these previous studies have indicated that the apparent pK_a of acids (or pK_b of bases) often increases when they are confined to surfaces. We are particularly interested in this phenomenon of reduced K_a and its relationship with the SAM surface charge state. We describe an experimental study where the force between a charged silica sphere attached to the AFM cantilever and the surface monolayer is used to deduce surface potential and charge (see Chart 1). These measurements indicate that the surface electrostatic potential of gold substrates derivatized with 3-mercaptopropionic acid is directly related to the fractional degree of acid dissociation. From the surface potential vs electrolyte pH data, the surface pK_a of the organic adsorbates is obtained from the theoretical model. To our knowledge, this is the first demonstration of AFM to measure the surface pK_a of surface-confined molecules.

Experimental Section

Reagents. The SAM species, 3-mercaptopropionic acid (Aldrich), was used as received. Solutions of KCl were freshly prepared from reagent grade chemical without further purification in 18 M Ω deionized water (Milli-Q Plus, Millipore Corp., Bedford, MA). The solution pH values were adjusted with 0.01

M KOH and 0.01 M HCl. Immediately before use, the solutions were deaerated with argon for 30 min.

Probe Preparation. Commercial silicon nitride cantilevers (Nanoprobe, Park Scientific, Mountain View, CA) with standard V-shape and square pyramidal tips were modified by attaching a silica sphere, as described by Ducker et al.^{11,14} The diameter of the silica spheres (Polysciences, Warrington, PA) was in the 10–20 μm range. In brief, the spherical particle was glued near the apex of the AFM cantilever under an optical microscope (Olympus, Model BHTU, Tokyo, Japan) with a low melting point epoxy resin (Epon 1002, Shell, Houston, TX). Care was taken to avoid coating the molten resin to the reflective gold side of the cantilever. A recent paper from Hillier et al.²⁵ gives more detailed procedures. Immediately prior to use, the spherical probe tip was rinsed with ethanol, rinsed with purified water, and then blown dry with argon.

Substrate Preparation. Commercial glass cover slips were used as silica substrates. Prior to measurement, the silica substrates were cleaned in a concentrated sulfuric/nitric acid solution followed by exposure to condensing steam vapor for 30 min. AFM images of the silica surfaces showed a mean roughness of 1.1 $\text{nm}/\mu\text{m}^2$ with a maximum peak to valley height of 3.7 nm over a 1 $\mu\text{m} \times 1 \mu\text{m}$ area.

To obtain smooth and reproducible force curves at different locations on a substrate, a very smooth substrate surface is needed. Large, flat, template-stripped gold surfaces were prepared by the procedure of Hegner et al.²⁶ Briefly, gold was vacuum deposited onto freshly cleaved mica sheets. AFM imaging of these vapor-deposited gold surfaces showed a mean roughness of 2.1 $\text{nm}/\mu\text{m}^2$ with a maximum peak to valley height of 19.5 nm over a 1 $\mu\text{m} \times 1 \mu\text{m}$ area. The vapor-deposited gold surface was then glued (Epo-tek No. 377, Polyscience) to a piece of Si wafer. After chemical stripping (in THF) of the gold from the mica, a remarkably smooth gold surface on Si was obtained. AFM imaging of this type of template-stripped gold surface indicated a mean roughness of 0.25 $\text{nm}/\mu\text{m}^2$ with a maximum peak to valley height of 2.7 nm over a 1 $\mu\text{m} \times 1 \mu\text{m}$ area. A scanning tunneling microscope was also employed to check the surface roughness. The freshly prepared template-stripped gold surface was immediately immersed in a 5 mM 3-mercaptopropionic acid ethanolic solution for over 12 h. Immediately before use, the SAM-covered gold substrate was rinsed with ethanol for 30 s and dried with a stream of argon.

Force Measurements. All force measurements were taken with a Digital Instruments (Santa Barbara, CA) Nanoscope III AFM. In these measurements, the force between a surface and the AFM tip is measured as a function of the distance between the surface and tip. Force measurements using standard cantilevers with square pyramidal tips showed behavior similar to that seen with the spherical probe but suffered from an ill-defined interaction radius, high noise, and poorly reproducible force data. The modified spherical tip has two significant advantages over the pyramidal tips. First, the larger tip surface area yields a higher signal-to-noise ratio (20–50 times) for the force measurements and smooth and reproducible force curves. Second, the geometry and size of the tip is well-characterized, so we could fit the force curves to DLVO theory to determine the surface potential.

The piezo scanner in the AFM had a maximum scan range of 15 $\mu\text{m} \times 15 \mu\text{m} \times 2 \mu\text{m}$. The scanner was calibrated in the *x* and *y* directions using a 1 \times 1 μm grid of gold on silicon and in the *z* direction by the method of Jaschke and Butt,²⁷ who measured the wavelength of the optical interference patterns resulting from reflection between the tip and a reflective substrate. All force measurements were conducted in a fluid cell (Digital Instruments) with Teflon tubing. Immediately before each experiment, the cell and tubing were cleaned by rinsing with EtOH, followed by copious amounts of purified water, and drying with argon.

The cantilever spring constant, *k*, was measured as in the earlier study,²⁵ by the method of Cleveland et al.,²⁸ from the change in cantilever resonant frequency with the addition of

(21) (a) Frisbie, C. D.; Rozsnyai, L. F.; Noy, A.; Wrighton, M. S.; Lieber, C. M. *Science* **1994**, *265*, 2071. (b) Noy, A.; Frisbie, C. D.; Rozsnyai, L. F.; Wrighton, M. S.; Lieber, C. M. *J. Am. Chem. Soc.* **1995**, *117*, 7943.
 (22) Thomas, R. C.; Houston, J. E.; Crooks, R. M.; Kim, T.; Michalske, T. A. *J. Am. Chem. Soc.* **1995**, *117*, 3830.
 (23) Bain, C. D.; Whitesides, G. M. *Langmuir* **1989**, *5*, 1370.
 (24) Bryant, M. A.; Crooks, R. M. *Langmuir* **1993**, *9*, 385.

(25) Hillier, A. C.; Kim, S.; Bard, A. J. *J. Phys. Chem.* **1996**, *100*, 18808.
 (26) Hegner, M.; Wagner, P.; Semenza, G. *Surf. Sci.* **1993**, *291*, 39.
 (27) Jaschke, M.; Butt, H.-J. *Rev. Sci. Instrum.* **1995**, *66*, 1258.
 (28) (a) Cleveland, J. P.; Manne, S.; Bocek, D.; Hansma, P. K. *Rev. Sci. Instrum.* **1993**, *64*, 403. (b) Sader, J. E.; Larson, I.; Mulvaney, P.; White, L. R. *Rev. Sci. Instrum.* **1995**, *66*, 3789.

Table 1. Surface Potential of the Silica Probe as a Function of Solution pH^a

solution pH	5.0	6.0	7.0	7.5	8.0	8.5	9.0	10.0	11.0
silica potential (mV)	-35	-43	-48	-50	-51	-52	-53	-53	-53

^a Force data were obtained between a silica sphere and a silica plate in 10^{-3} M KCl aqueous solutions of different pH at 25 °C. The interaction between two silica surfaces is repulsive and can be well-reproduced (except at short distances) by DLVO theory. The force data, when fit to the sum of repulsive electrostatic and attractive van der Waals interactions with $A_H = 0.88 \times 10^{-20}$ J, provide the silica surface potential and Debye length of $\kappa^{-1} = 9.63$ nm.

known end masses. When the added mass is plotted against the inverse square of the cantilever resonant frequency, the slope gives the cantilever spring constant. This method gave a spring constant of $k = 0.65 \pm 0.12$ N/m; the manufacturer's nominal value was 0.58 N/m.

During the acquisition of a force curve, the measured experimental parameters were the cantilever deflection, obtained from the voltage of the sectored photodiode detector, and the substrate z displacement, which was given by the piezo scanner voltages. The raw data giving the tip deflection vs substrate displacement were converted to a normalized force (force/radius) F/R vs tip-substrate separation, d , from knowledge of the scanner calibration, cantilever spring constant, and tip radius. The zero force position was determined from the static tip deflection at large separations. Zero separation was defined as the onset of constant compliance or contact region. The absolute force was calculated from the change in cantilever position by Hooke's law and the cantilever spring constant.

Results and Discussion

Theory. For the interaction between identically charged surfaces, the theory of colloidal stability of DLVO²⁹ separates the total interaction free energy into two components: an attractive van der Waals interaction energy (V_A) and an attractive or repulsive electrostatic force (V_E). There is also some evidence for an additional repulsion (V_S) at small separations arising from the presence of ordered solvent layers.³⁰ Thus, the total interaction free energy is simply the sum $V_A + V_E + V_S$.

When AFM force measurements are conducted between two colloidal spheres (radii R_1 and R_2) or a colloidal sphere and a flat surface, the Derjaguin approximation is employed.³¹ This approximation, which holds when the sphere radii are much larger than the intersphere separation, relates the interaction free energy per unit area between parallel plates to the force (F) between spheres of effective radius R_T , where

$$1/R_T = 1/R_1 + 1/R_2 \quad (1)$$

The force between spheres is given by the expression

$$F/R_T = 2\pi(V_A + V_E + V_S) \quad (2)$$

The van der Waals energy (V_A) can be expressed, ignoring the effect of retardation, by an equation of the form

$$V_A = -A_H/12\pi d^2 \quad (3)$$

where A_H is the Hamaker constant and d is the distance of closest approach between the sphere and the plate. The Hamaker constant is a function of the dielectric properties of the two surfaces and the intervening medium and is typically 10^{-19} – 10^{-21} J.³²

To calculate the electrical double layer interaction energy (V_E), the potential distribution must be known. For similarly charged surfaces at low surface potentials, the linearized form of the Poisson–Boltzmann equation yields the same results as the DLVO theory. For dissimilarly charged surfaces, the effect of an additional Maxwellian stress term that represents an induced image charge cannot be neglected. In these cases, the complete nonlinear Poisson–Boltzmann equation must be solved,

which can only be accomplished by numerical techniques.³³ In this work, the electrical double-layer interaction was calculated for the constant-potential or constant-charge limits of the nonlinear Poisson–Boltzmann equation using the method of Hillier et al.²⁵ who used a finite element discretization of the equation with linear basis functions.

Force Measurements. The surface potential of the silica sphere as a function pH was determined by measuring F/R vs d curves between the sphere and a silica (glass) substrate, as described earlier.^{14,34,35} The results are shown in Table 1 and details are given in the supporting information.

A study of the interaction forces with the adsorbed species on surfaces requires knowledge of the force–distance curves for the clean surface as a blank to compare with the film-covered surface. This measurement also yields information on the cleanliness of the surface and the sphere surface roughness. To calculate the interaction between the silica sphere and gold surface in aqueous solution, A_H must be known. A_H values have been measured before for both the silica–silica^{14,36} and gold–gold³⁷ interactions. A_H values reported for silica–silica interactions in aqueous solution are 0.88×10^{-20} to 2.2×10^{-20} J. A_H values reported for gold–gold interactions in aqueous solution are 2.5×10^{-19} to 4.0×10^{-19} J. From these reported A_H values, the geometric mean for silica–gold interactions is $A_H = 4.7 \times 10^{-20}$ to 9.4×10^{-20} J. These calculated values can be compared to experimentally measured values with freshly prepared, template-stripped, clean gold surfaces. Figure 1 shows a purely attractive silica–gold interaction force curve in deionized water (pH ≈ 6.0) with the best fit to a parabolic, nonretarded van der Waals interaction (eq 3). For the silica–gold interaction in aqueous solution, the best fit curve gives $A_H = 1.1 \times 10^{-19}$ J. A_H can also be determined from the snap-in distance through the following equation²⁵

$$d_{\text{snap}} = (A_H R_T / 3k)^{1/3} \quad (4)$$

where the snap-in distance, d_{snap} , is a function of A_H , the tip radius, R_T , and the cantilever spring constant, k . For $R_T = 8.0 \mu\text{m}$, $k = 0.65$ mN/m, and $d_{\text{snap}} = 8.65$ nm, a silica–gold interaction $A_H = 1.6 \times 10^{-19}$ J is obtained. The influence of electrostatic forces between silica and gold cannot be completely eliminated when measuring A_H in

(29) (a) Derjaguin, B. V. *Trans. Faraday Soc.* **1940**, *36*, 203. (b) Derjaguin, B. V.; Landau, L. D. *Acta Phys. Chem.* **1941**, *14*, 633. (c) Derjaguin, B. V.; Landau, L. D. *J. Exp. Theor. Phys.* **1941**, *11*, 802. (d) Verwey, E. J. W.; Overbeek, J. T. G. *Theory of the Stability of Lyophobic Colloids*; Elsevier: New York, 1948.

(30) (a) Overbeek, J. T. G. *J. Chem. Phys.* **1987**, *87*, 4406. (b) Ise, N. *Angew. Chem., Int. Ed. Engl.* **1986**, *25*, 323. (c) Schmitz, K. S. *Acc. Chem. Res.* **1996**, *29*, 7.

(31) Derjaguin, B. V. *Kolloid Z.* **1934**, *69*, 155. (32) (a) Lifshitz, E. M. *Sov. Phys.-JETP* **1956**, *2*, 73. (b) Dzyaloshinskii, I. E.; Lifshitz, E. M.; Pitaevskii, L. P. *Sov. Phys.-JETP* **1960**, *37*, 165.

(33) (a) Chan, D. Y. C.; Pashley, R. M.; White, L. R. *J. Colloid Interface Sci.* **1980**, *77*, 283. (b) McCormack, D.; Carnie, S. L.; Chan, D. Y. C. *J. Colloid Interface Sci.* **1995**, *169*, 177.

(34) Grabbe, A.; Horn, R. G. *J. Colloid Interface Sci.* **1993**, *157*, 375. (35) Meagher, L.; Pashley, R. M. *Langmuir* **1995**, *11*, 4019.

(36) (a) Horn, R. G.; Smith, D. T.; Haller, W. *Chem. Phys. Lett.* **1989**, *162*, 404. (b) Peschel, G.; Belouschek, P.; Muller, M. M.; Muller, M. R.; Konig, R. *Colloid Polym. Sci.* **1982**, *260*, 444. (c) Rabinovich, Y. I.; Derjaguin, B. V.; Churaev, N. *Adv. Colloid Interface Sci.* **1982**, *16*, 63.

(37) (a) Schrader, M. E. *J. Colloid Interface Sci.* **1984**, *100*, 372. (b) Rabinovich, Y. I.; Churaev, N. V. *Russ. J. Phys. Chem.* **1990**, *52*, 256.

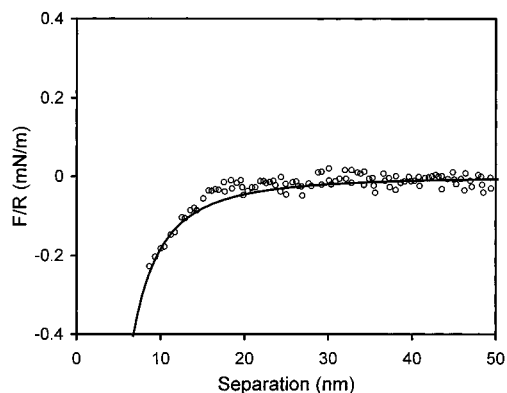


Figure 1. Force between silica probe ($R = 8.0 \mu\text{m}$) and freshly prepared template-stripped gold surface in deionized water at 25°C and $\text{pH} \approx 6.0$. Attractive force is fit to van der Waals attraction of $F/R = -A_H/6d^2$ and the snap-in distance ($d_{\text{snap}} = 8.65 \text{ nm}$) to eq 4. In aqueous solution, the silica–gold interaction gave $A_H = 1.1 \times 10^{-19}$ and $1.6 \times 10^{-19} \text{ J}$ using the curve fit and snap-in distance, respectively.

water. Under the solution pH conditions, the silica surface is negatively charged, and the potential of the gold surface is determined by solution composition and specifically adsorbed ions. At open circuit, the potential of gold should be near the potential of zero charge. However, any specifically adsorbed positive or negative ions on the gold surface would result in an error in this measurement of A_H . On the other hand, the negatively charged silica probe can induce an image charge at the gold surface as the probe approaches the gold surface. The observed attractive force between silica and clean gold in aqueous solutions suggests that the gold surface was either originally uncharged or slightly positively charged; the measured value for A_H would be slightly overestimated in the latter case. Finally, the snap-in phenomenon prevents accurate measurement of forces existing at separations of less than the snap-in distance. In fact, this is one of the limitations in using the passive cantilever, especially for attractive interaction force measurements.

With the self-assembled monolayers of 3-mercaptopropionic acid-covered gold, the formation of hydrogen bonds between the terminal carboxylic acid groups probably facilitates compact monolayer formation.³⁸ In this case, only the monolayer surface contacts the aqueous solution when a compact monolayer has been achieved. The interaction between a silica probe and carboxylic acid-terminated SAM-covered gold substrate was a strong function of the pH of the electrolyte. In aqueous solutions containing 10^{-3} M KCl , we obtained pH-dependent force–separation curves (Figure 2) that were reproducible on changing either from high to low pH or vice versa. Below pH 6.0 there were no measurable long range electrostatic interactions between silica and the SAM-covered gold substrate, suggesting that the gold substrate was uncharged; i.e., at $\text{pH} < 6$, the terminal carboxylic acid group remained completely protonated. The electrostatic repulsive force increased with an increase in pH between 6.0 and 10.0, indicating that the surface carboxylic acid was gradually deprotonated as the pH increased. Above pH 10.0 the electrostatic repulsive force no longer increased with an increase of solution pH, showing that the surface charge remained constant above pH 10.0. Because these repulsive forces are well below the force load limit and above the force detection limit of the cantilever used, any increasing repulsive force due to the increasing surface charge would be experimentally measurable above pH

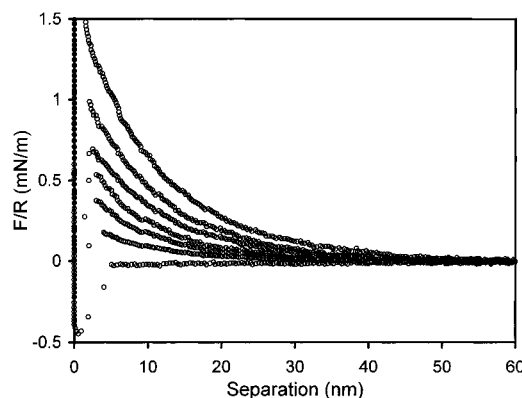


Figure 2. Force between silica probe ($R = 8.0 \mu\text{m}$) and carboxylic acid-terminated SAM-covered gold substrate in 10^{-3} M KCl solutions at 25°C as a function of solution pH. The curves correspond to pH values, from bottom to top, of 6.0, 7.0, 7.5, 8.0, 8.5, 9.0, and 10.0. Electrostatic repulsion increases as the solution pH increases from 6.0 to 10.0.

10.0, implying that the terminal carboxylic acid is fully dissociated near pH 10.0.

The change in double-layer force with pH between the negative silica tip and the SAM-covered gold substrate can be explained in terms of both the properties of the double layer and the fractional degree of acid dissociation at the gold substrate. The diffuse double layer near the gold substrate is probed by the spherical silica tip as it moves through the double layer, which consists of counterions that compensate the charge residing at the gold–SAM/solution interface. Below pH 6.0 where the surface $-\text{COOH}$ groups are fully protonated, no diffuse double layer forms in the solution, and there are no measurable double-layer forces. From pH 6.0 to 10.0, the surface acid dissociates with increasing solution pH, so that the net surface charge of the substrate becomes negative and a diffuse double layer with a net positive charge forms. This diffuse layer consists of a higher local concentration of K^+ (and H^+) and a lower local concentration of Cl^- (and OH^-). Thus, the repulsive force between the negatively charged silica probe and the monolayer-covered gold substrate increases with pH (Figure 2, upper curves).

To calculate the surface electrostatic potentials (ψ) of the monolayers of carboxylic acid, the force data were compared to theoretical predictions of the forces between dissimilarly charged surfaces obtained by solving the complete nonlinear Poisson–Boltzmann equation.²⁵ In Figure 3, we show the results of theoretical curves fit to experimental force data at selected pH values in 10^{-3} M KCl solutions. These calculations include both electrostatic and van der Waals interactions, with $A_H = 1.1 \times 10^{-19} \text{ J}$ and $\kappa^{-1} = 9.63 \text{ nm}$. In all cases, the theoretical results (solid curves) represent a good fit to the force data (open circles) at separations of greater than 10 nm. The upper curve (thick line) is for the model with boundary conditions constrained to a constant surface charge at both the probe and substrate, while the lower curve (thin line) is at a constant surface potential. Note that the theoretical models deviate severely from the measured data at separations of less than 10 nm. There are several factors that are probably responsible for this deviation: the inaccuracy of the measured A_H value, the ill-defined location for the plane of surface charge due to roughness of the silica probe and gold substrate, and the exclusion of the solvent repulsion term from the theoretical curves. Nevertheless, in each data set, the fit with a constant surface charge condition to the data is better than that with a constant surface potential condition. In Figure 3a, the force curve at pH 7.0, the best fit, with the known silica probe surface potential of $\psi_p = -48 \text{ mV}$, gives a

(38) Yang, H. C.; Dermody, D. L.; Xu, C.-J.; Ricco, A. J.; Crooks, R. M. *Langmuir* **1996**, *12*, 726.

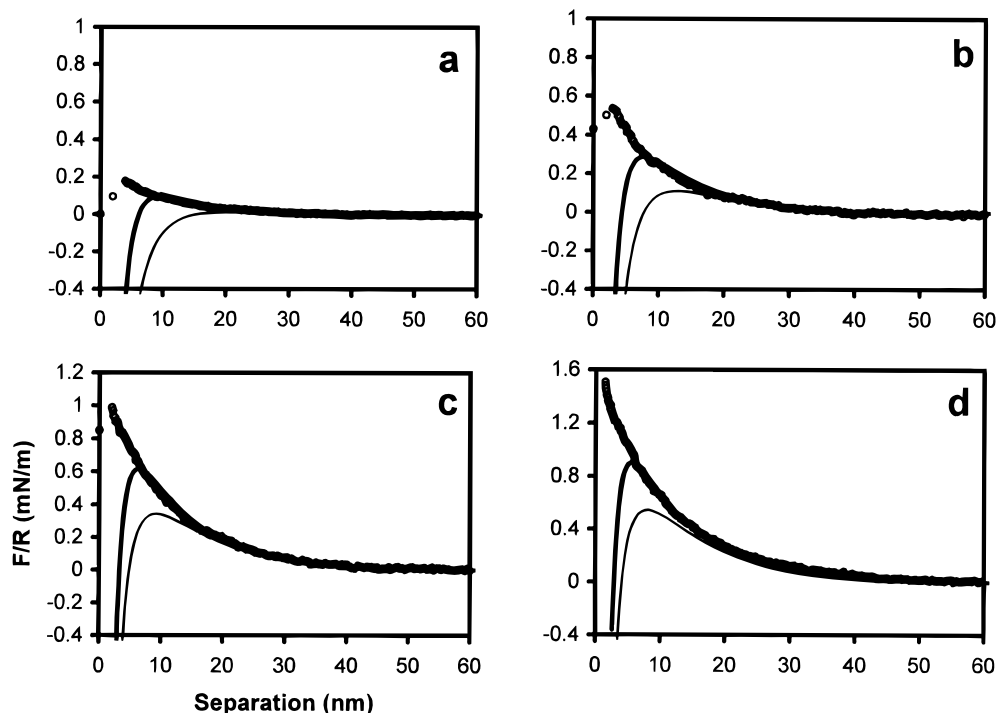


Figure 3. Measured (circles) and theoretical (solid lines) force between silica sphere and carboxylic acid-terminated SAM-covered gold substrate at constant charge (thick line) and constant potential (thin line) in aqueous 10^{-3} M KCl solutions at 25 °C and different pH values. In each fit, $A_H = 1.1 \times 10^{-19}$ J and $\kappa^{-1} = 9.63$ nm. ψ_s = substrate surface potential, ψ_p = probe surface potential. (a) pH 7.0, $\psi_p = -48$ mV, $\psi_s = -12$ mV; (b) pH 8.0, $\psi_p = -51$ mV, $\psi_s = -28$ mV; (c) pH 9.0, $\psi_p = -53$ mV, $\psi_s = -48$ mV; (d) pH 10.0, $\psi_p = -53$ mV, $\psi_s = -62$ mV.

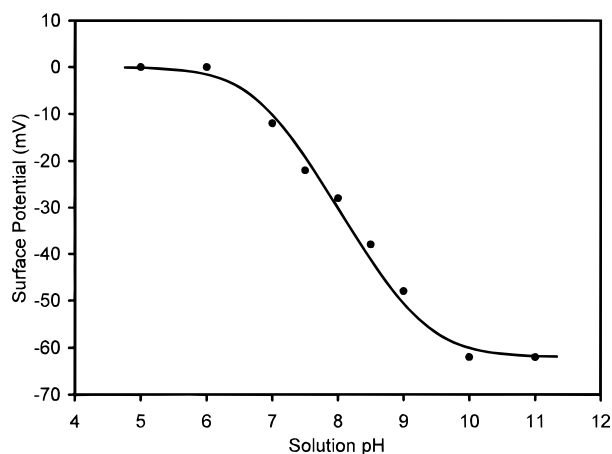


Figure 4. Measured (solid circles) and theoretical (solid line) surface potentials of the monolayer of carboxylic acid in 10^{-3} M KCl solutions at 25 °C as a function of solution pH. Surface potential values in addition to those given in the caption of Figure 3: pH 5.0, $\psi_s = 0$ mV; pH 6.0, $\psi_s = 0$ mV; pH 7.5, $\psi_s = -22$ mV; pH 8.5, $\psi_s = -38$ mV; pH 11.0, $\psi_s = -62$ mV. The best theoretical fit gives surface pK_a at pH 7.7.

surface electrostatic potential of the SAM-covered gold substrate of $\psi_s = -12$ mV. The best fit parameters for other force data are given in the caption of Figure 3.

With knowledge of the surface electrostatic potential of the surface-confined monolayer $-\text{COOH}$ groups at different solution pH values, we find a correlation between the surface potential and solution pH. The results (solid circles) are given in Figure 4. The sigmoidal shape of the plot suggests the surface potential of the SAM-covered gold substrate is pH dependent. Since these surface potentials are directly related to the fractional degree of surface carboxylic acid dissociation, Figure 4 can be viewed as a direct surface acid titration curve. There are two main features in this titration curve. First, the apparent $pK_{1/2}$ (the solution pH at which the surface potential is midway between its plateau at high and low pH) of the

adsorbed carboxylic acid is near pH 8.0, which is about 3.5 units higher than the pK_a measured for similar acids in bulk aqueous solution.³⁹ Second, the titration curve is much broader (extending from pH 6.0 to 10.0) than those observed for monocarboxylic acids in aqueous solutions. These findings are in good agreement with previous results for similar systems by different methods.^{5,23}

The large increase in surface pK_a as compared to the solution value can be attributed to strong intermolecular lateral hydrogen bonding among the surface molecules, which has been shown spectroscopically to produce a significant shift of the IR-active carbonyl stretching mode toward lower energy.⁴⁰ Thus hydrogen bond formation causes the acidic protons to be held more tightly on the monolayer surface. Moreover, deprotonation of an acid layer is energetically unfavorable because of the large electrostatic repulsion that the neighboring ionized carboxylate groups experience at the monolayer/solution interface.

To explain the broadening of the titration curve, a theoretical model which accounts for the effect of surface potential on ψ vs pH data is needed. The acid–base equilibrium properties of surface confined acids have been studied for lipophilic compounds that are spread at the air–water interface by taking the electrostatic contribution into consideration.⁴¹ More recently, Smith and White⁴² revisited these systems and proposed a theoretical model that relates the differential capacitance of metal electrodes coated with monolayer films of a molecular acid or base to the applied potential and solution pH. Their theoretical model can be applied to the analysis of ψ vs pH data. Briefly, the basis of this model is as follows. The

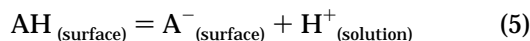
(39) Lide, D. R. *CRC Handbook of Chemistry and Physics*, 71st ed.; CRC Press: Boca Raton, FL, 1990.

(40) Crooks, R. M.; Sun, L.; Xu, C.; Hill, S. L.; Ricco, A. *J. Spectrosc.* **1993**, *8*, 28.

(41) Caspers, J.; Goormaghtigh, E.; Ferreira, J.; Brasseur, R.; Vandenberghe, M.; Ruyschaert, J.-M. *J. Colloid Interface Sci.* **1983**, *91*, 546.

(42) Smith, C. P.; White, H. S. *Langmuir* **1993**, *9*, 1.

monolayer of carboxylic acid (AH) at the solid/liquid interface contacts a solution at different pH values, so that the following surface reaction occurs:



The equilibrium constant of this surface reaction is given by

$$K_a = \frac{f}{1-f} [\text{H}^+]_s \quad (6)$$

where f is the fraction of surface acid dissociated and $[\text{H}^+]_s$ is the H^+ concentration at the surface. $[\text{H}^+]_s$ is related to the bulk H^+ concentration, $[\text{H}^+]_\infty$, through a Boltzmann distribution⁴¹

$$[\text{H}^+]_s = [\text{H}^+]_\infty e^{-e\psi/kT} = [\text{H}^+]_\infty e^{-F\psi/RT} \quad (7)$$

where e is the electronic charge, F the Faraday constant, k the Boltzmann constant, R the molar gas constant, and ψ the electrostatic potential at the surface. From eq 6, it follows that

$$\text{p}K_a = \text{pH}_s - \log \frac{f}{1-f} \quad (8)$$

where pH_s is given (eq 7) by

$$\text{pH}_s = \text{pH}_\infty + \frac{\psi}{2.303RT/F} \quad (9)$$

where pH_∞ is the solution pH. The combination of eqs 8 and 9 gives^{41,42}

$$\log \frac{f}{1-f} = \text{pH} - \text{p}K_a + \frac{\psi}{2.303RT/F} \quad (10)$$

Equation 10 is the theoretical model relating surface electrostatic potential ψ and the degree of ionization of the surface acid groups. If the electrostatic contribution ($F\psi/2.303RT$) is not included, eq 10 becomes the same equation as that for acid–base equilibrium in bulk aqueous solutions.

The electrostatic potential associated to the monolayer is given by the Gouy–Chapman theory of the electrical double layer. In this work, ψ was determined from the double-layer force measurements. The monolayer surface charge, σ , is related to ψ by the following relationship⁴³

$$\sigma = \epsilon_0 \epsilon_s \kappa (2kT/e) \sinh\left(\frac{e\psi}{2kT}\right) \quad (11)$$

where $\kappa = e(2r^0/\epsilon_0\epsilon_s kT)^{1/2}$ is the inverse Debye length of the electrolyte solution with the dielectric constant ϵ_s , which is taken to be 78.49 and assumed to be pH-independent, r^0 is the bulk number density of monovalent cations from the inert and pH-determining electrolyte, and ϵ_0 is the permittivity of free space. In 10^{-3} M KCl solution, the Debye length (κ^{-1}) of the double layer was experimentally determined to be 9.63 nm.

The experimental results indicate that complete surface acid dissociation occurs near pH 10.0 at which the maximum surface electrostatic potential ($\psi_m = -62$ mV) and charge (σ_m) is reached, while the surface acid remains totally undissociated near pH 6.0 where the minimum surface potential is 0 mV. So, with a given ψ between 0 and -62 mV, the monolayer surface charge (σ) can be

calculated. Since the fractional degree of acid dissociation is directly related to surface charge, it can be determined by

$$f = \sigma/\sigma_m = \sinh[e\psi/2kT]/\sinh[e\psi_m/2kT] \quad (12)$$

Therefore, the only parameter needed to fit the ψ vs pH theoretical curve to the measured data is the $\text{p}K_a$ value. Figure 4 shows the best fit (solid line) to the experimental data with a surface $\text{p}K_a$ of 7.7. As shown, the theoretical model not only yields the surface $\text{p}K_a$ value but also provides experimental evidence to support the effect of surface charge on the extent of ionization; that is, the electrostatic interactions at the monolayer/solution interface produce a broader titration curve.

Conclusions

An AFM was used to measure the double-layer forces between a silica probe and either silica or carboxylic acid-terminated SAM-covered gold substrates in the presence of aqueous KCl solutions. The silica–silica interaction was repulsive and was used to determine the surface potential of the silica probe as a function of pH. The interaction between silica and a clean gold surface exhibited an attractive interaction at neutral pH. The interaction between silica and a SAM-covered gold substrate was a strong function of solution pH. Theoretical fits of the force data to solutions of the complete nonlinear Poisson–Boltzmann equation yield the surface electrostatic potentials of the surface-confined monolayers of carboxylic acid. The constant surface charge condition more accurately reflects the force data at surface separations above 10 nm. The surface potential of the monolayer with $-\text{COOH}$ groups is directly related to the fractional degree of surface acid dissociation. By correlation of the surface potential to the solution pH, a surface carboxylic acid titration curve was obtained. The fit of the theoretical model to the titration curve provides the surface $\text{p}K_a$ value and experimental evidence to support a model where the broadening of the titration curve is attributed to electrostatic interactions at the monolayer/solution interface.

Force measurements between an electrode surface and a tip of known geometry and charge in an AFM can provide quantitative information about the surface charge on an electrode immersed in solution and under potential control. This is useful in studying modification of electrode surfaces, e.g., with multilayer films applied sequentially. Monitoring of film growth currently relies on ellipsometric or electrochemical measurements. Surface charge measurements via AFM supply a complementary method. Studies of this type are currently under way in this laboratory.

Acknowledgment. The support of this research by grants from the Robert A. Welch Foundation and the National Science Foundation (CHE-9508525) is gratefully acknowledged. The authors also thank Dr. F.-R. F. Fan for helpful discussions and Dr. Andrew C. Hillier (University of Virginia) for providing the computer program for the calculation of double-layer forces.

Supporting Information Available: Details of the force measurements between silica probe and substrate (2 pages). See any current masthead page for ordering information and Internet access instructions.

(43) Bard, A. J.; Faulkner, L. R. *Electrochemical Methods*; Wiley: New York, 1980.